Spin-Dependent Electronic States of the Ferromagnetic Semimetal EuB_6

Xiaohang Zhang,[1] Stephan von Molnár,[1] Zachary Fisk,[2] and Peng Xiong[1]
[1]*Department of Physics and MARTECH, Florida State University, Tallahassee, Florida 32306, USA*
[2]*Department of Physics, University of California, Irvine, California 92697, USA*
(Received 19 December 2007; published 22 April 2008)

The spin polarization of EuB_6 has been measured by using Andreev reflection spectroscopy. Analyses of the conductance spectra of the EuB_6/Pb junctions yield a spin polarization of about 56%. The results demonstrate that the ferromagnetic EuB_6 is not half-metallic. Combined with the Hall effect and magnetoresistivity data, the results indicate a semimetallic band structure with a fully spin-polarized hole band and an unpolarized electron band. The values and the spread of the measured spin polarization are *quantitatively* consistent with the experimentally determined Fermi surface and carrier densities.

DOI: 10.1103/PhysRevLett.100.167001 PACS numbers: 74.50.+r, 71.20.−b, 75.25.+z

The hexaboride compounds are a group of materials with a similar body-centered-cubic-like crystal structure but disparate and intriguing electronic and magnetic properties. Tight-binding band structure calculations [1] indicate that the B_6 octahedra can be regarded as anions with a charge of -2. Therefore, unlike the trivalent hexaborides, the electronic structure of divalent hexaborides is expected to be more complicated and ambiguous due to the balance in valence. Band structure calculations [2,3] suggest that the electronic properties of divalent hexaborides depend critically on the details of the band structure in the vicinity of the X point. Slight variations in the interatomic distances between the nearest B atoms may cause changes from a semimetal to a semiconductor. EuB_6 is the most intensively studied divalent hexaboride due to its unusual ferromagnetism and electronic transport and, especially, the intricate interplay between them. Two consecutive phase transitions were observed at 15.3 and 12.5 K, respectively [4], which were initially interpreted as two different ferromagnetic orderings. However, later Raman scattering studies [5] and magnetic and transport measurements [6] showed that the one at 15.3 K is essentially a charge delocalization transition via the overlap of magnetic polarons. Despite much work, the band structure of EuB_6 remains in debate. A semimetallic structure was widely accepted primarily due to the observed metallic character of the electronic transport over a broad temperature range. Early band structure calculations [3] with local density approximation (LDA) indicate that EuB_6 is a semimetal with a small overlap of the conduction band (CB) and the valence band (VB) at the X point. The results of both de Haas–van Alphen (dHvA) [7,8] and Shubnikov–de Haas (SdH) [8] measurements were consistent with this picture, revealing small ellipsoidal pockets of electrons and holes centered at the X points. On the other hand, angle-resolved photoemission spectroscopy (ARPES) measurements [9] at a temperature of 20–30 K point to a semiconductor band structure with an X-point gap >1 eV. Previous low field Hall effect (HE) and magnetoresistance (MR) measurements [10,11] imply a semiconductor to semimetal transition accompanied by the ferromagnetic ordering. Recent optical conductivity spectroscopy measurements over a wide spectral range [12], however, appear to contradict these conclusions and support the semimetallic picture even in the paramagnetic state. Furthermore, the spin occupation of the bands in the ferromagnetic state remains controversial. Recent calculations with the LDA + U and Kondo-lattice models [13,14] predict that EuB_6 is a *half-metallic* semimetal: Large spontaneous Zeeman splittings for both CB and VB result in an energy gap for the spin-down states, an enhanced overlap for the spin-up states, and thus complete spin polarization (P) for the charge carriers. In contrast, earlier LDA calculations [3] yield significant band splitting for CB only, which would result in an overall P of $\sim$50%.

The aim of the present work is to directly probe P of the EuB_6 by using Andreev reflection (AR) [15] spectroscopy. We measured P of around 56% with a spread of $\pm$9%, which clearly demonstrates that EuB_6 is not a half-metal. The results, together with analysis of the HE and MR data, present a semimetallic band structure with complete spin polarization in the *valence* band only. This picture and the relatively simple Fermi surface of EuB_6 [8] enable us to, for the first time, directly calculate the transport spin polarizations [16] of a ferromagnet and compare with the experimental data.

EuB_6/Pb planar junctions, as depicted schematically in Fig. 1, were prepared and P values were derived from AR spectroscopy measurements. Single crystals of EuB_6 were grown from an aluminum flux as described in an earlier paper [17]. The junctions were made on platelet-shaped specimens with a thickness of about 0.3 mm and varied dimensions from $\sim 1 \times 1$ to $\sim 2 \times 4$ mm^2. Laue x-ray diffraction indicates that the platelet surface and the edges are along a $\langle 001 \rangle$ or equivalent axis of a cubic structure. To fabricate a junction, an EuB_6 single crystal was precleaned in NaOH solution followed by rinsing with deionized water to remove any flux residue. The crystal was then soldered onto an indium stripe on a microscope cover slide with the bottom surface of the crystal completely covered by in-

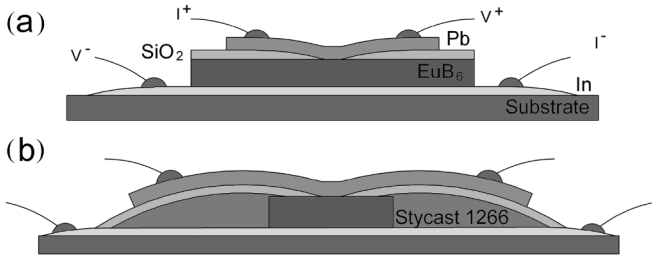

FIG. 1. Schematic view of the junction structure. (a) General structure of an EuB_6/Pb junction; (b) Stycast 1266 is used to accommodate small crystals.

dium. To define the contact region between EuB_6 and Pb, a 50 nm-thick layer of SiO_2 was sputter-deposited on the top surface of the single crystal through a shadow mask, leaving a gap of 0.1 mm. A 0.1 mm-wide Pb stripe with a thickness of about 500 nm was then thermally evaporated across the gap. For some small crystals, we used Stycast 1266 epoxy to extend beyond the size of the crystal as shown in Fig. 1(b).

The zero-bias junction resistance versus temperature (R_J versus T) and the conductance spectra (dI/dV versus V) were measured in a ^{3}He cryostat by using phase-sensitive lock-in detection. The normal state junction resistances of our samples varied from several Ohms to about 100 Ω. The residual resistivity of EuB_6 is very small, as shown in the left inset in Fig. 2. Specifically, for the EuB_6 specimens used, the contribution from the crystal is calculated to be less than 0.2 Ω. The EuB_6/In contact is at least 100 times larger than the EuB_6/Pb junction. More importantly, the R_J versus T curves (one is shown in Fig. 2) always clearly

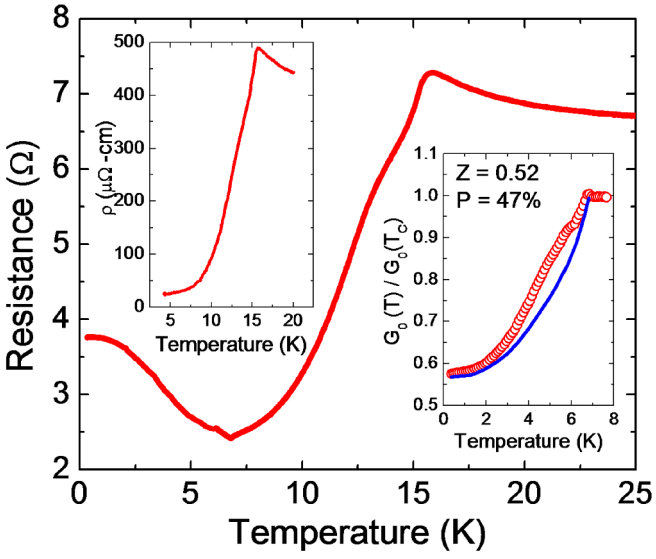

FIG. 2 (color online). Junction resistance as a function of temperature. Left inset: Resistivity of an EuB_6 crystal at low temperatures. Right inset: Temperature dependence of the normalized conductance of an EuB_6/Pb junction (circles) and a theoretical curve based on the spin-polarized BTK theory (solid line).

reflected the superconducting transition of Pb at ~7 K but did not exhibit any features at the In transition (3.4 K). Therefore, the measured R_J is dominated by the EuB_6/Pb junction. The conductance spectrum of a normal-metal/superconductor (N/S) junction is well described by the theory of Blonder, Tinkham, and Klapwijk (BTK) [18], in which the spectrum is determined by the barrier strength, described by a dimensionless parameter Z. For ferromagnet/superconductor (FM/S) junctions, the conductance spectrum is modified by the suppression of AR due to the spin imbalance in the FM [19]. The fitting of the modified spectrum, with Z and P as the fitting parameters, thus gives reliable determination of P for the FM [20].

Figures 3(a) and 3(b) show the normalized conductance spectra of an EuB_6/Pb junction at two different temperatures. The normalization of each curve was based on a corresponding sweep at a magnetic field slightly higher than the critical field of the Pb film. Figure 3(a) shows the spectrum measured at 1.4 K and the best fit to the spin-polarized BTK model. The actual measurement temperature (1.4 K) and an expected energy gap (Δ) value of 1.32 meV were used in the fitting. The best fit yields $Z = 0.52$ and $P = 47\%$ with a certainty better than 2%. Figure 3(b) shows the spectrum of the same sample at 0.35 K. Without changing any parameters used in fitting the spectrum at 1.4 K, a spin-polarized BTK conductance curve was generated with $T = 0.35$ K. The theoretical curve matches the experimental data very well [Fig. 3(b)]. The consistency in the obtained P and Z values is expected because both parameters should be temperature-independent in this range. Finally, theoretical values of the normalized zero-bias conductance at different temperatures were calculated from the spin-polarized BTK model with $Z = 0.52$ and $P = 47\%$ (right inset in Fig. 2): There is good agreement between the calculated values and the experimental data over the entire temperature range.

Similar measurements and analyses were performed on seven different EuB_6/Pb junctions, and the P values obtained are 47%, 64%, 57%, 56%, 58%, 54%, and 65%, which cluster around 56% with a spread of approximately ±9%. The Z values of the junctions cover a relatively broad range from 0.29 to 1.0. There is no apparent correlation between P and Z, and we did not observe any

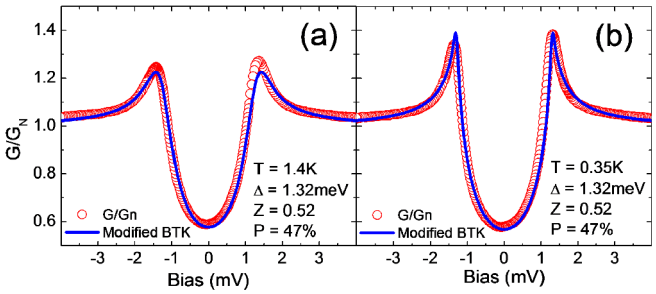

FIG. 3 (color online). Normalized conductance spectra for the EuB_6/Pb junction at (a) 1.4 and (b) 0.35 K; solid lines are modified BTK fits.

indication of the decline of P with increasing Z, consistent with our previous observations in other planar junctions [21] and in contrast to the effect often seen in point contact experiments [22]. The results are in clear contradiction with the half-metallic picture as a possible outcome of the LDA + U calculations [13,14]. With a two-pocket Fermi surface [7,8], P near 50% is consistent with the picture of one band being fully spin-polarized while the other is unpolarized. A fully polarized CB is the scenario predicted by earlier LDA calculations [3]. However, the opposite situation with a fully polarized VB is also possible.

In order to further clarify the spin-dependent band structure of EuB_6, we carried out MR and HE measurements on a $4.0 \times 2.2 \times 0.1$ mm^3 platelet from the same batch. The data are shown in Figs. 4(a) and 4(b). The MR, which peaks around T_c, becomes positive below T_c. In Fig. 4(b), there appear to be two temperature regimes where the Hall slope takes on two distinct values, with a large (small) Hall slope for high (low) temperatures. At intermediate temperatures, there is a transition from the large slope to the small slope with increasing applied field, and the switching field decreases with decreasing temperature. Qualitatively similar features in the MR and HE were observed by Wigger *et al.* [11]. The switch in the Hall slope with decreasing temperature across T_c and with increasing field, as well as the changes from negative to positive MR, could be associated with a coalescing of magnetic polarons [5] and charge delocalization [6]. The inset in Fig. 4(b) shows the Hall resistivity at low temperatures. With the exception of the appearance of quantum oscillations at the lowest temperatures, both the MR and the HE show negligible temperature dependence below 5.6 K. Therefore, regardless of the high temperature variations, the band structure of EuB_6 becomes stabilized at low temperatures, with little temperature or field dependence.

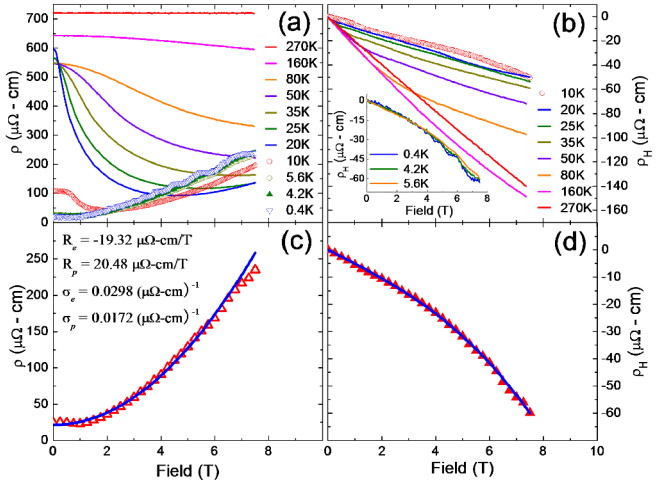

FIG. 4 (color online). (a) Magnetoresistivity and (b) Hall resistivities measured at different temperatures with fields up to 7.5 T; the inset in (b) shows the HE below 5.6 K; (c) and (d) show two-band model fits (solid lines) for the MR and HE (triangles), respectively, at 5.6 K; the fitting parameters are listed in (c).

With the stability at low temperatures, we use the standard two-band model to simultaneously describe the MR and the Hall coefficient [23]:

$$\rho = \frac{\sigma_e + \sigma_p + \sigma_e\sigma_p(\sigma_e R_e{}^2 + \sigma_p R_p{}^2)B^2}{(\sigma_e + \sigma_p)^2 + \sigma_e{}^2\sigma_p{}^2(R_e + R_p)^2B^2}, \quad (1)$$

$$R_H = \rho_H/B = \frac{R_e\sigma_e{}^2 + R_p\sigma_p{}^2 + \sigma_e{}^2\sigma_p{}^2R_eR_p(R_e + R_p)B^2}{(\sigma_e + \sigma_p)^2 + \sigma_e{}^2\sigma_p{}^2(R_e + R_p)^2B^2}, \quad (2)$$

where R_e, R_p, σ_e, and σ_p are the Hall coefficients and conductivity for the electrons and holes, respectively. To eliminate the influence of the small kink of MR at low fields and the oscillations at high fields, we fit the curves for 5.6 K in a magnetic field range from 2.0 to 6.0 T and then plotted the fits in the entire field range, as shown in Figs. 4(c) and 4(d). Obviously, there is excellent agreement for both curves. The fitting parameters are listed in Fig. 4(c). From the resulting Hall coefficients for electrons and holes, we obtain the carrier density for each band: $n_e = 3.23 \times 10^{19}$ cm^{-3} and $n_p = 3.05 \times 10^{19}$ cm^{-3}, respectively. These values are close to the carrier densities obtained through two-band analysis by Wigger *et al.* [11]; especially, the n_e/n_p ratio is almost the same.

In the paramagnetic phase, the low field Hall coefficients $R_H|_{B=0}$ indicate an electronlike effective carrier density of $n_{\text{eff}} = 2.70 \times 10^{19}$ cm^{-3} in zero field. With a semiconducting band structure, these carriers would all be electrons; the holes in the ferromagnetic phase at low temperatures would have to come from a spin splitting of the VB with the spin-up branch crossing the chemical potential. In this scenario, however, all missing electrons in the VB would end up in the CB; hence, the electron-hole imbalance would be the same in both phases. This is clearly contradicted by the n_e and n_p at low temperatures determined above. We therefore conclude that EuB_6 has a semimetallic band structure even in the paramagnetic phase. In this picture, with comparable R_e and R_p, the dominance of electrons in the HE implies that $\sigma_p/\sigma_e \ll 1$, which suggests localization of the holes in the paramagnetic phase. A natural conclusion from this observation is that it is the localized *holes* that form the bound magnetic polarons via exchange interaction with the Eu^{2+}. At low temperatures and/or high fields, the alignment of the Eu^{2+} moments leads to overlap of the magnetic polarons and delocalization of the holes and, consequently, a large spin splitting of the VB. This conclusion is corroborated by the results of Goodrich *et al.* [7], who identified the hole pocket as spin-polarized based on their analysis of the amplitude of the quantum oscillations. Further, a substantial splitting of the VB was recently observed directly

through ARPES [24]. Taken together, the measured spin polarization and the analyses of HE and MR strongly suggest semimetallic band structures for EuB_6 in both paramagnetic and ferromagnetic phases; in the ferromagnetic state, a large spontaneous Zeeman splitting of the valence band leads to fully spin-polarized holes and unpolarized electrons.

This picture provides a physical model from which quantitative calculation of P is possible based on the experimentally determined ellipsoidal pockets of electrons and holes. As pointed out by Mazin [16], P measured by AR spectroscopy not only has to do with the density of states (DOS) at the Fermi level but also depends on the size and shape of the Fermi surface. In particular, for an Andreev junction in the diffusive limit (as in our case), the measured P corresponds to a value with spin densities weighted by $v^2_{F\uparrow(\downarrow)}$:

$$P_{Nv^2} = (\langle Nv^2\rangle_\uparrow - \langle Nv^2\rangle_\downarrow)/(\langle Nv^2\rangle_\uparrow + \langle Nv^2\rangle_\downarrow), \quad (3)$$

where N is the DOS at the Fermi surface and v the Fermi velocity. Starting from the Fermi surface of EuB_6 mapped out by quantum oscillation measurements [7,8], we calculate P_{Nv^2} and compare with the measured values here.

Although there were slight inconsistencies between different experiments, various dHvA [7,8] and SdH [8] measurements have identified an electron and a hole ellipsoid pocket centered at the X point, each with a pair of frequencies corresponding to the minimum and maximum extremal areas of the ellipsoids. From the angular dependence of the frequencies, Aronson *et al.* [8] were able to determine the volumes of the electron and hole pockets and, consequently, electron and hole densities of 1.20×10^{20} and 2.03×10^{20} cm^{-3}, respectively. The densities were calculated without considering any spin polarization. If the larger pocket is populated by spin-up holes only and the smaller pocket is equally occupied by spin-up and spin-down electrons, the results of Ref. [8] then yield hole and electron densities of 1.01×10^{20} and 1.20×10^{20} cm^{-3}, respectively, much closer to full compensation. With this quantitative picture, we calculate P_{Nv^2} by integrating over the entire Fermi surface and obtain $P_{Nv^2} = 49.8\%$. On the other hand, the two-band model fits to our low temperature HE and MR data yielded carrier densities of 3.23×10^{19} and 3.05×10^{19} cm^{-3} for electrons and holes, respectively. With a fully polarized VB and an unpolarized CB, and by maintaining the shapes of the two ellipsoidal pockets of Aronson *et al.* [8], these densities result in $P = 53\%$.

Because of the small Fermi surface and intrinsic carrier densities ($\sim 10^{-3}$ per unit cell) in EuB_6, small fluctuations in sample stoichiometry can lead to sizable changes in electron and hole densities as well as the extent of the inequalities between them. Previous quantum oscillation [7,8] and HE [11] measurements have revealed such variations. Variations in the degree of compensation change the relative sizes of the electron and hole pockets and, consequently, the overall P. In fact, a small variation of the degree of compensation can account for the spread in the P values we observed: Based on the band structure we have deduced and the shapes of the measured ellipsoidal electron and hole pockets by Aronson *et al.* [8], the range of P values corresponds to n_p/n_e from 0.75 ($P = 47\%$) to 1.28 ($P = 65\%$).

In summary, the spin polarization of EuB_6 crystals has been determined by AR spectroscopy, and the obtained values are in the range of 56% ($\pm$ 9%), which directly contradicts the half-metallic band structure. The results of spin polarization, transport, and Fermi surface measurements provide a quantitatively consistent picture in agreement with a semimetallic band structure with a substantial band splitting for the valence band only in the ferromagnetic state.

The authors thank R. Goodrich, J. Denlinger, and J. Allen for useful discussions and Jun Lu for acquiring x-ray diffraction data. This work was supported by a FSU Research Foundation PEG grant (P. X. and S. v. M.) and NSF Grants No. DMR-0710492 and No. DMR-0503360 (Z. F.).

[1] H. C. Longuet-Higgins and M. de V. Roberts, Proc. R. Soc. A **224**, 336 (1954).
[2] A. Hasegawa and A. Yanase, J. Phys. C **12**, 5431 (1979).
[3] S. Massidda *et al.*, Z. Phys. B **102**, 83 (1997).
[4] T. Fujita *et al.*, Solid State Commun. **33**, 947 (1980); L. Degiorgi *et al.*, Phys. Rev. Lett. **79**, 5134 (1997).
[5] P. Nyhus *et al.*, Phys. Rev. B **56**, 2717 (1997).
[6] S. Süllow *et al.*, Phys. Rev. B **62**, 11 626 (2000).
[7] R. G. Goodrich *et al.*, Phys. Rev. B **58**, 14 896 (1998).
[8] M. C. Aronson *et al.*, Phys. Rev. B **59**, 4720 (1999).
[9] J. D. Denlinger *et al.*, Phys. Rev. Lett. **89**, 157601 (2002).
[10] C. N. Guy *et al.*, Solid State Commun. **33**, 1055 (1980).
[11] G. A. Wigger *et al.*, Phys. Rev. B **69**, 125118 (2004).
[12] J. H. Kim *et al.*, arXiv:cond-mat/0703266.
[13] J. Kuneš and W. E. Pickett, Phys. Rev. B **69**, 165111 (2004).
[14] M. Kreissl and W. Nolting, Phys. Rev. B **72**, 245117 (2005).
[15] A. F. Andreev, Sov. Phys. JETP **19**, 1228 (1964).
[16] I. I. Mazin, Phys. Rev. Lett. **83**, 1427 (1999).
[17] Z. Fisk *et al.*, J. Appl. Phys. **50**, 1911 (1979).
[18] G. E. Blonder *et al.*, Phys. Rev. B **25**, 4515 (1982).
[19] M. J. M. de Jong and C. W. J. Beenakker, Phys. Rev. Lett. **74**, 1657 (1995).
[20] R. J. Soulen, Jr. *et al.*, Science **282**, 85 (1998); S. K. Upadhyay *et al.*, Phys. Rev. Lett. **81**, 3247 (1998).
[21] J. S. Parker *et al.*, Phys. Rev. Lett. **88**, 196601 (2002); C. Ren *et al.*, Phys. Rev. B **75**, 205208 (2007).
[22] G. T. Woods *et al.*, Phys. Rev. B **70**, 054416 (2004).
[23] S. M. Watts *et al.*, Phys. Rev. B **61**, 9621 (2000).
[24] J. Denlinger, APS March Meeting, http://meetings.aps.org/link/BAPS.2007.MAR.A7.3 (2007).